Wiley
Advances in Mathematical Physics
Volume 2025, Article ID 3604476, 18 pages
https://doi.org/10.1155/admp/3604476

WILEY

Research Article

On the Study of Nonlinear Murray Equation in Non-Newtonian Fluids: Fractional Solitary Wave Structures, Chaos, and Sensitivity Demonstration

J. Muhammad[1], **U. Younas**[1], **Haroon**[2], **H. Mukalazi**[3], **M. E. Meligy**[4] and **K. A. Alnowibet**[5]

[1]*Department of Mathematics, Shanghai University, No. 99 Shangda Road, Shanghai, China*
[2]*College of Forestry and Landscape Architecture, South China Agricultural University, Guangzhou, China*
[3]*Department of Mathematics and Statistics, Faculty of Science, Kyambogo University, Kampala, Uganda*
[4]*Jadara University Research Center, Jadara University, Irbid, Jordan*
[5]*Statistics and Operations Research Department, College of Science, King Saud University, Riyadh, Saudi Arabia*

Correspondence should be addressed to U. Younas; usmanalgebra@shu.edu.cn and H. Mukalazi; hmukalazi@kyu.ac.ug

Received 12 January 2025; Revised 24 September 2025; Accepted 25 September 2025

Academic Editor: Shikha Binwal

This article introduces fractional solitary wave structures to the nonlinear Murray equation by applying advanced techniques, namely the generalized Arnous method and the modified generalized Riccati equation mapping method (MGREMM). This equation is known as a generalization of the nonlinear reaction–diffusion equation, which describes the diffusion of chemical reactions in a medium. For such equations, solitary wave solutions are of the utmost importance in numerical and analytical theories. Despite the widespread use of numerical methods, a deeper understanding of the dynamics requires the enhancement of analytical methods used to derive analytical solutions. In order to achieve the desired solutions, the governing equation is transformed into an ordinary differential equation by utilizing an appropriate wave transformation with the β-derivative. The solitary wave solutions of various types, such as mixed, singular, dark, bright, bright–dark, and combined solitons, are extracted. Additionally, we plot a variety of graphs with various parameters to examine the solution's behavior at various parameter values. Moreover, another important aspect of this study is to discuss the chaotic and sensitivity analysis of the studied model by the assistance of the Galilean transformation. The 2D phase portraits, Poincaré maps, time series analysis, and sensitivity analysis graphs based on the initial conditions have been sketched. This study achieves a significant milestone by applying the aforementioned methods with the assistance of β-fractional derivatives to the proposed equation for the first time and contributes significantly to the existing literature. In many fields, the equation in concern can introduce improved algorithms that model the evolution of certain types of biological and physical systems, particularly in contexts like vascular network growth and fluid dynamics. By demonstrating the effectiveness of the applied approaches, the outcomes of this research could improve understanding of the nonlinear dynamic properties shown by the given system.

Keywords: β-fractional derivatives; chaotic and sensitivity analysis; generalized arnous method; modified generalized riccati equation mapping method; nonlinear murray equation; solitons

1. Introduction

In recent years, finding solitary wave solutions to various kinds of nonlinear evolution equations (NLEEs) has been an essential problem in many branches of mathematics and physics. Most natural phenomena arising in nonlinear science, including optical fibers, fluid mechanics, chemical reactions, nuclear physics, plasma, physics and ecology, biology, can be modeled and described by nonlinear partial differential equations (NLPDEs) [1, 2]. Interesting nonlinearities in nature have

attracted scholars, who see nonlinear science as the most advantageous field for advancing our understanding of the universe. The mathematical characterization of complex systems with time-varying properties necessitates the study of multiple NLPDEs, and for advanced, accurate results closely relating to experimental results, nonlinear fractional partial differential equations (FNLPDEs) play a vital role [3]. It is common practice for researchers to reinterpret many dynamical phenomena as NLPDEs. Consequently, in recent years, the research of NLPDEs has constantly attracted significant attention. Different scientific methods of investigation are embodied by nonlinear differential equations. Analytical and numerical solutions to the models are necessary to understand the inherent properties of the nonlinear models. Using symbolic computations, researchers have devised many effective techniques to guarantee the correctness of soliton solutions to NLPDEs [4].

Soliton theory is a core concept that forms the basis of certain mathematical and physical techniques used to analyze a specific category of NLPDEs, known as evolution equations, and exhibits a distinct type of basic solution. These solutions, called solitons, behave like particles after interacting with one another; they take the shape of localized waves that maintain their characteristics. A soliton is defined by physics and mathematics as a self-sustaining wave packet that travels at a constant speed without changing its form. A variety of solitons, including bright, dark, peakons, kink, anti-kink, spatiotemporal, temporal, spatial, and singular. Many investigations have shown the various characteristics of soliton solutions as well as their potential applications in technical and scientific realms [5, 6]. Nonlinear optics, plasma physics, fluid dynamics, communications engineering, and coastal engineering are among the numerous disciplines in which soliton solutions are utilized. They are essential in the promotion of global communication, considered a critical advancement. Mathematicians have employed intricate numerical and analytical techniques to identify soliton solutions for various systems. Consequently, soliton waves are becoming more significant in several domains, including optical fibers, ferromagnetic materials, and nonlinear optics. Combining physics, mathematics, and computer science in this way illustrates how scientific study is always evolving to address practical problems. Research into these fields and potential new uses may benefit from a better grasp of soliton waves.

Exact solutions are considered to be of great significance in a variety of physical systems, as they facilitate the investigation of physical behaviors and provide a foundation for further study and research. The only way to acquire an exact solution for any physical system is to characterize its behaviors as an ODE or PDE. NLPDEs or FNLPDs can be used to model the majority of industrial complexes or natural phenomena. Many academics developed a wide range of methods and approaches in an attempt to discuss the scientific problems. Following are some of the most well-known and often used newly developed techniques: Hirota bilinear method [7], multiple exp-function approach [8], extended hyperbolic auxiliary equation method [9], power-exponential function method [10], Riccati equation mapping method [11], Adomian decomposition technique [12], Darboux transformation [13], Bernoulli $\frac{G'}{G}$-expansion method [14], bifurcation analysis [15], $\frac{G'}{G}$-expansion method [16], modified simple equation technique [17], iterative transform method [18], Sardar subequation method [19], $\tan(\frac{\phi}{2})$ technique [20], simplest equation technique [21], and others like [22–26].

Moreover, a dynamical system is an equation that depicts the evolution of a system through time. This system's constituent differential equations describe the time-dependent behavior of the system. Many fields use dynamic systems to study the behavior of complex systems. These fields include engineering, biology, economics, ecology, physics, and engineering. Basic dynamical systems include the stock market, the planets in a solar system, the motion of a pendulum, and the dynamics of a species' population [27]. In addition, the chaos theory delves into the study of deterministic systems that, although being controlled by basic mathematical equations, display intricate and surprising behavior [28]. Even small changes to the starting conditions can have a big impact on the final outcome. The phase space of the system is finally defined by the path taken by neighboring points. An infinite number of periodic orbits are densely packed into the system's phase space. Some well-known examples of chaotic systems include the fluid movement, the logistic map, weather, and the double pendulum. Numerous disciplines have made use of chaos theory, including the social sciences, economics, engineering, biology, and physics. It has changed the way we think about deterministic systems and how we perceive natural randomness and predictability [29]. Instead of illustrating the entire trajectory, the Poincaré maps, also known as Poincaré sections, emphasize the points at which the trajectory intersects the plane, thereby offering a more comprehensive understanding of potential bifurcations, stability features, and periodic orbits. This methodology provides a comprehensive visualization of the system's dynamics, enabling the identification of stability characteristics, periodicity, and transitions to more intricate behaviors [30].

So, the equation under investigation has not been explored by applying the proposed techniques, despite a comprehensive review of the existing literature. Consequently, this study aims to employ the suggested analytical methodology known as the generalized Arnous method [31] and the new modified generalized Riccati equation mapping method (MGREMM) [32], and analyzing its dynamical behavior to understand the complex dynamic behaviors of the nonlinear Murray equation. Non-Newtonian behavior, blood flow, and vessel wall elasticity are all factors that are considered by the nonlinear Murray equation. The actual form of the nonlinear Murray equation may differ based on the model's assumptions and inputs. A power law relationship between flow rate and vessel diameter is integrated in certain formulations of the equation, while others employ more complex dynamic behaviors.

The structure of the article is arranged as follows: the basic properties for the fractional derivative are investigated in Section 2. The proposed model is introduced in Section 3, while the proposed methods are employed to calculate soliton solutions in Section 4. Plots of the obtained solutions are included in Section 5. The chaotic and sensitivity analyses are presented in Sections 6 and 7, respectively. The conclusion is offered in Section 8.

2. Fractional Order Derivatives

Significant attention has been paid to the subject of fractional calculus and its applications by researchers. Use of fractional differential equations (FDEs) is an organized and practical approach to elucidating natural phenomena. Among multiple disciplines, including plasma physics, solid physics, control theory, data processing, electrode electrolyte polarization, biogenetics, electromagnetic waves, and glass fiber, FPDEs are of significant importance. The literature has presented various efficient and reliable FPDEs, such as M-truncated derivative [33], and conformable derivative [34] for solitary wave solutions. Recent studies in fractional calculus have shown that models based on fractional orders are often more reliable than models based on integer orders in terms of exactly reflecting real physical occurrences. The β-derivative is a generalized operator that effectively captures the memory and hereditary properties of complex systems through a tunable parameter, making it highly relevant in modeling non-Newtonian fluids. It offers enhanced flexibility in representing anomalous diffusion and nonlinear stress–strain relationships, which are typical in such media. Beyond physics, β-derivatives have also found applications in financial modeling, where they support risk management, portfolio optimization, and market timing by allowing investors to adjust for systematic risk and dynamic market behavior. In both fields, the β-derivative's ability to account for memory effects and nonlinear dynamics makes it a powerful tool for accurately modeling real-world phenomena. Using the suggested model as an example, this study evaluates the efficiency of fractional derivatives for understanding and exploring certain physical behaviors.

2.1. The β-Derivative

Definition 1. For $\kappa(t):[c,\infty)\to\mathbb{R}$, the β-derivative [35] is defined by the following:

$$\mathscr{D}_t^{\beta}\{\kappa(t)\}=\lim_{\varepsilon\to 0}\frac{\kappa\left(t+\varepsilon\left(t+\frac{1}{\Gamma(\beta)}\right)^{1-\beta}\right)-\kappa(t)}{\varepsilon},\ 0<\beta\le 1. \tag{1}$$

Theorem 1. *See [35], suppose that κ and $h\neq 0$ are β-differentiable functions such that $0<\beta\le 1$. Then,*

1. $\mathscr{D}_t^{\beta}(c\{\kappa(t)\}+d\{h(t)\})=c\mathscr{D}_t^{\beta}\{\kappa(t)\}+d\mathscr{D}_t^{\beta}\{h(t)\}$, for all $c,\ d\in\mathbb{R}$.
2. $\mathscr{D}_t^{\beta}(\{h(t)\}\times\{\kappa(t)\})=\{\kappa(t)\}\mathscr{D}_t^{\beta}(\{h(t)\})+\{h(t)\}\mathscr{D}_t^{\beta}(\{\kappa(t)\})$.
3. $\mathscr{D}_t^{\beta}(\frac{\{\kappa(t)\}}{\{h(t)\}})=\frac{\{h(t)\}\mathscr{D}_t^{\beta}\{\kappa(t)\}-\{\kappa(t)\}\mathscr{D}_t^{\beta}\{h(t)\}}{(\{h(t)\})^2}$.
4. $\mathscr{D}_t^{\beta}\{\kappa(t)\}=\frac{d\{\kappa(t)\}}{dt}(t+\frac{1}{\Gamma(\beta)})^{1-\beta}$.
5. If c is a constant, then $\mathscr{D}_t^{\beta}\{c(t)\}=0$.

3. The Governing Equation

In medical theory, Murray's law or principle describes the relationship between blood artery width and blood flow rate. A mathematical formulation known as the nonlinear Murray equation considers the influence of fluid dynamics, geometry, and other relevant factors on blood flow. It can be described as follows:

$$R^3=C_1\left(\frac{Q}{w}\right)^2+D_1\left(\frac{w}{L}\right), \tag{2}$$

where L symbolizes the vessel's length, the parameters C_1 and D_1 are real constants. The letter R represents the blood vessel radius; Q stands for the blood flow rate through the vessel. The convection term is incorporated into the nonlinear reaction–diffusion equation [36, 37], which is expressed as follows:

$$u_t=A(u)u_{xx}+B(u)u_x+C_2(u), \tag{3}$$

where the function $u=u(x,t)$ is unknown and the functions $A(u),\ B(u), C_2(u)$ are chossen as arbitrary smooth functions. Taking $A(u)=1, B(u)=\gamma_1 u$, and $C_2(u)=\gamma_2 u-\gamma_3 u^2$, where $\gamma_1,\ \gamma_2,\ \gamma_3\in\mathbb{R}$, then Equation (3), read [38, 39] as follows:

$$\mathscr{D}_t^{\beta}u=\mathscr{D}_{xx}^{2\beta}u+\gamma_1 u\mathscr{D}_x^{\beta}u+\gamma_2 u-\gamma_3 u^2, \tag{4}$$

where Equation (4) is known as the extended β-fractional form of the nonlinear Murray equation. The parameters γ_1, γ_2, γ_3 play distinct roles in shaping the dynamics of the solution, particularly in pattern formation, biological population dynamics, or nonlinear diffusion models. The term $\gamma_1 u\mathscr{D}_x^{\beta}u$ introduces nonlinear convection or advection. It models self-steepening or nonlinear transport effects, where the movement of the quantity u depends on its own magnitude and its gradient. Where the term $\gamma_2 u$ contributes to linear growth or decay, for $\gamma_2>0$ indicates source-like behavior such as population growth, energy input, while for $\gamma_2<0$ implies damping or decay. Similarly, for $\gamma_3 u^2$ represents nonlinear damping, intraspecific competition, or resource limitation. It restricts unbounded growth caused by the $\gamma_2 u$ term and introduces a saturation mechanism.

Equation (4) has practical application, such that in pattern formation, it helps explain how spatial structures such as stripes, spots, or waves emerge in chemical and biological systems, including animal coat patterns and morphogenesis. In biological population dynamics, the equation models how populations spread, interact, and stabilize, capturing effects like traveling population waves, predator–prey interactions, and the persistence or extinction of species under nonlinear constraints. In nonlinear diffusion models, it is used to describe transport processes where diffusion is not constant but depends on concentration or density, such as tumor growth, the spread of epidemics, or chemical reactions in heterogeneous media. By combining nonlinearity with diffusion, the Murray equation provides a powerful framework for predicting self-organization and dynamic behaviors across diverse scientific fields. Moreover, unlike classical models, the fractional Murray equation incorporates memory and long-range dependencies through fractional calculus. This allows it to more accurately capture

the complexities of biological growth and anomalous diffusion, where past conditions and spatial correlations significantly impact current system behavior, resulting in better alignment with empirical data.

In addition, the soliton solutions of Equation (4) are investigated employing various techniques, such as in [38], different types of solutions are studied with the analytical technique known as the modified extended direct algebraic method, where in [39] Bernoulli wavelet collocation method is used to extract the soliton solutions. We calculate the numerous solutions of the proposed model in the subsequent section.

Moreover, in our research, solitary wave structures of the nonlinear Murray equation were obtained using the generalized Arnous method and the MGREMM. The generalized Arnous method yielded a wider variety of mixed and singular solitons, while MGREMM provided clearer parametric families with simpler amplitude-speed relations. Both produced bright, dark, bright-dark, and combined soliton solutions. By applying a Galilean transformation, we explored the system's chaotic dynamics and sensitivity to initial conditions, confirmed through phase portraits, Poincaré maps, time-series, and sensitivity analyses, which revealed regions of stability, periodicity, and chaos influenced by the fractional order and parameter choices.

4. Mathematical Analysis

We proceed with the assumption for Equation (4) as follows:

$$u = \Phi(\xi); \tag{5}$$

$$\xi = \frac{k}{\beta}\left(x + \frac{1}{\Gamma(\beta)}\right)^{\beta} - \frac{v}{\beta}\left(t + \frac{1}{\Gamma(\beta)}\right)^{\beta}, \ (\text{for } \beta\text{-derivative}) \tag{6}$$

where the symbols k is an arbitrary constant and v is the wave speed. The following nonlinear ODE is obtained by implementing the aforementioned transformations in Equation (4):

$$k^2\Phi''(\xi) + \gamma_1 k\Phi(\xi)\Phi'(\xi) + v\Phi'(\xi) - \gamma_3\Phi(\xi)^2 + \gamma_2\Phi(\xi) = 0. \tag{7}$$

Moreover, we have to use the advised approaches to solve Equation (7). Additionally, using the balancing principle between the terms Φ^2 and Φ'' in Equation (7) results in $n = 2$.

4.1. Solutions via Generalized Arnous Method. The generalized Arnous approach [31] has the solution as follows:

$$\Phi(\xi) = \alpha_0 + \sum_{r=1}^{n} \frac{\alpha_r}{(\psi(\xi))^r} + \sum_{r=1}^{n} \frac{\beta_r(\psi'(\xi))^r}{(\psi(\xi))^r}. \tag{8}$$

When $n = 2$, we have the following:

$$\Phi(\xi) = \alpha_0 + \frac{\alpha_1}{\psi(\xi)} + \frac{\alpha_2}{(\psi(\xi))^2} + \beta_1\frac{\psi'(\xi)}{\psi(\xi)} + \beta_2\left(\frac{\psi'(\xi)}{\psi(\xi)}\right)^2, \tag{9}$$

where the letters α_0, α_1, α_2, β_1, β_2 are constants and the function $\psi(\xi)$ is given by the following:

$$(\psi'(\xi))^2 = (\psi(\xi)^2 - \rho)\ln(\delta)^2, \tag{10}$$

where

$$\psi^{(n)}(\xi) = \begin{cases} \psi'(\xi)\ln(\delta)^2, & n \text{ is odd}, \\ \psi(\xi)\ln(\delta)^2, & n \text{ is even}, \end{cases}$$

for $\delta > 0$, $\delta \neq 1$ and $n \geq 2$. The solution of Equation (10) is subsequently provided as follows:

$$\psi(\xi) = A\ln(\delta)\delta^{\zeta} + \frac{\rho}{4A\ln(\delta)\delta^{\xi}}, \tag{11}$$

where the parameters A and ρ are arbitrarily chosen. The general solutions are as follows when Equation (9) is combined with Equation (10) in Equation (7).

Set-1 $\alpha_0 = \frac{\gamma_2}{\gamma_3} - \beta_2\log^2(\delta)$, $\alpha_1 = 0$, $\beta_1 = 0$, $\alpha_2 = \beta_2\rho\log^2(\delta)$.

The solitary wave solution for set-1 is as follows:

$$u_1(x,t) = \frac{\beta_2\rho\log^2(\delta)}{\left(\frac{\rho\delta^{-\xi}}{4A\log(\delta)} + A\delta^{\xi}\log(\delta)\right)^2} + \frac{\beta_2\left(A\delta^{\xi}\log^2(\delta) - \frac{\rho\delta^{-\xi}}{4A}\right)^2}{\left(\frac{\rho\delta^{-\xi}}{4A\log(\delta)} + A\delta^{\xi}\log(\delta)\right)^2} - \beta_2\log^2(\delta) + \frac{\gamma_2}{\gamma_3}, \tag{12}$$

with $\delta = e$ and $\rho = 4A^2$, in Equation (12), we get the bright–dark soliton solution as follows:

$$u_2(x,t) = \beta_2\tanh^2(\xi) + \beta_2\operatorname{sech}^2(\xi) - \beta_2 + \frac{\gamma_2}{\gamma_3}. \tag{13}$$

In the same way, the combined soliton solution (12) for $\delta = e$ and $\rho = -4A^2$, is given by the following:

$$u_3(x,t) = \beta_2\coth^2(\xi) - \beta_2\operatorname{csch}^2(\xi) - \beta_2 + \frac{\gamma_2}{\gamma_3}. \tag{14}$$

Set-2 $\alpha_0 = \frac{\gamma_2}{2\gamma_3} - \beta_2\log^2(\delta)$, $\alpha_1 = 0$, $\beta_1 = \frac{\gamma_2}{2\gamma_3\log(\delta)}$, $\alpha_2 = \beta_2\rho\log^2(\delta)$, $k = \frac{\gamma_1\gamma_2}{4\gamma_3\log(\delta)}$, $v = -\frac{\gamma_2(\gamma_2\gamma_1^2 + 4\gamma_3^2)}{8\gamma_3^2\log(\delta)}$.

Solutions for set-2 are as follows:

$$u_4(x,t)=\frac{\beta_2\rho\log^2(\delta)}{\left(\frac{\rho\delta^{-\xi}}{4A\log(\delta)}+A\delta^{\xi}\log(\delta)\right)^2}+\frac{\beta_2\left(A\delta^{\xi}\log^2(\delta)-\frac{\rho\delta^{-\xi}}{4A}\right)^2}{\left(\frac{\rho\delta^{-\xi}}{4A\log(\delta)}+A\delta^{\xi}\log(\delta)\right)^2}+\frac{\gamma_2\left(A\delta^{\xi}\log^2(\delta)-\frac{\rho\delta^{-\xi}}{4A}\right)}{2\gamma_3\log(\delta)\left(\frac{\rho\delta^{-\xi}}{4A\log(\delta)}+A\delta^{\xi}\log(\delta)\right)}-\beta_2\log^2(\delta)+\frac{\gamma_2}{2\gamma_3}, \tag{15}$$

with $\delta=e$ and $\rho=4A^2$, the solution (15) in combo bright-dark soliton solution is expressed as follows:

$$u_5(x,t)=\beta_2\tanh^2(\xi)+\beta_2\operatorname{sec}h^2(\xi)-\beta_2+\frac{\gamma_2\tanh(\xi)}{2\gamma_3}+\frac{\gamma_2}{2\gamma_3}. \tag{16}$$

In the same way, the solution (15) for $\delta=e$ and $\rho=-4A^2$ in the combined singular soliton solution may be written as follows:

$$u_6(x,t)=\beta_2\cot h^2(\xi)-\beta_2\operatorname{csc}h^2(\xi)-\beta_2+\frac{\gamma_2\cot h(\xi)}{2\gamma_3}+\frac{\gamma_2}{2\gamma_3}, \tag{17}$$

where ξ is defined in Equation (6).

4.2. Solutions via MGREMM. General solution for MGREMM [32] is described by the following:

$$\Phi(\xi)=a_0+\sum_{r=1}^{n}a_r\Omega^r(\xi)+\sum_{r=1}^{n}\psi_r(\xi)\left(\frac{\Omega'(\xi)}{\Omega(\xi)}\right)^r. \tag{18}$$

When $n=2$, we have the following:

$$\Phi(\xi)=a_0+a_1\Omega(\xi)+a_2\Omega^2(\xi)+\psi_1(\xi)\frac{\Omega'(\xi)}{\Omega(\xi)}+\psi_2(\xi)\left(\frac{\Omega'(\xi)}{\Omega(\xi)}\right)^2, \tag{19}$$

and $\Omega'(\xi)=\delta_0+\delta_1\Omega(\xi)+\delta_2\Omega(\xi)^2$. A variety of solutions are as follows when Equation (19) is inserted into Equation (7):

(I): For $\delta_1^2-4\delta_0\delta_2>0$, $\delta_1\delta_2\neq0$, $\delta_0\delta_2\neq0$, and $a_0=\frac{\gamma_2\left(\frac{\gamma_3\delta_1}{\sqrt{\gamma_3^2(\delta_1^2-4\delta_0\delta_2)}}+1\right)}{2\gamma_3}$, $a_1=\frac{\gamma_2\delta_2}{\sqrt{\gamma_3^2(\delta_1^2-4\delta_0\delta_2)}}$, $\psi_1=0$, $\psi_2=0$, $a_2=0$, $k=-\frac{\gamma_1\gamma_2}{2\sqrt{\gamma_3^2(\delta_1^2-4\delta_0\delta_2)}}$, $\nu=\frac{\gamma_2(\gamma_2\gamma_1^2+4\gamma_3^2)}{4\gamma_3\sqrt{\gamma_3^2(\delta_1^2-4\delta_0\delta_2)}}$, we have the following solutions:

The dark soliton solution is as follows:

$$u_1(x,t)=\left(\frac{\gamma_2\left(\frac{\gamma_3\delta_1}{\sqrt{\gamma_3^2\left(\delta_1^2-4\delta_0\delta_2\right)}}+1\right)}{2\gamma_3}-\frac{\gamma_2\left(\sqrt{\delta_1^2-4\delta_0\delta_2}\tanh\left(\frac{1}{2}\sqrt{\delta_1^2-4\delta_0\delta_2}\xi\right)+\delta_1\right)}{2\sqrt{\gamma_3^2(\delta_1^2-4\delta_0\delta_2)}}\right). \tag{20}$$

The explicit solitary wave solution is as follows:

$$u_2(x,t)=\left(\frac{\gamma_2\left(\frac{\gamma_3\delta_1}{\sqrt{\gamma_3^2\left(\delta_1^2-4\delta_0\delta_2\right)}}+1\right)}{2\gamma_3}-\frac{\gamma_2\left(\sqrt{\delta_1^2-4\delta_0\delta_2}\cot h\left(\frac{1}{2}\sqrt{\delta_1^2-4\delta_0\delta_2}\xi\right)+\delta_1\right)}{2\sqrt{\gamma_3^2(\delta_1^2-4\delta_0\delta_2)}}\right). \tag{21}$$

The combined bright–dark soliton solution is as follows:

$$u_3(x,t)=\left(\frac{\gamma_2\left(\frac{\gamma_3\delta_1}{\sqrt{\gamma_3^2\left(\delta_1^2-4\delta_0\delta_2\right)}}+1\right)}{2\gamma_3}-\frac{\gamma_2\left(\delta_1+\sqrt{\delta_1^2-4\delta_0\delta_2}\left(\tanh\left(\sqrt{\delta_1^2-4\delta_0\delta_2}\xi\right)+i\sec h\left(\sqrt{\delta_1^2-4\delta_0\delta_2}\xi\right)\right)\right)}{2\sqrt{\gamma_3^2(\delta_1^2-4\delta_0\delta_2)}}\right). \tag{22}$$

The solitary wave solution is as follows:

$$u_4(x,t)=\left(\frac{\gamma_2\left(\frac{\gamma_3\delta_1}{\sqrt{\gamma_3^2\left(\delta_1^2-4\delta_0\delta_2\right)}}+1\right)}{2\gamma_3}-\frac{\gamma_2\left(\sqrt{\delta_1^2-4\delta_0\delta_2}\left(\cot h\left(\sqrt{\delta_1^2-4\delta_0\delta_2}\xi\right)+\operatorname{csch}\left(\sqrt{\delta_1^2-4\delta_0\delta_2}\xi\right)\right)+\delta_1\right)}{2\sqrt{\gamma_3^2(\delta_1^2-4\delta_0\delta_2)}}\right). \tag{23}$$

When $a_0=-\frac{2\delta_0\delta_2\psi_2^2-\delta_1\psi_2\sqrt{(\delta_1^2-4\delta_0\delta_2)\psi_2^2}+\sqrt{(\delta_1^2-4\delta_0\delta_2)^2\psi_2^4}}{2\psi_2}$, $a_1=\delta_2(\sqrt{(\delta_1^2-4\delta_0\delta_2)\psi_2^2}-\delta_1\psi_2)$, $a_2=-\delta_2^2\psi_2$, $\psi_1=-\sqrt{(\delta_1^2-4\delta_0\delta_2)\psi_2^2}-\delta_1\psi_2$, $\gamma_2=-\frac{6k^2\sqrt{(\delta_1^2-4\delta_0\delta_2)^2\psi_2^4}}{\psi_2^2}$, $\gamma_3=\frac{6k^2}{\psi_2}$, $\gamma_1=0$, $\nu=\frac{5k^2\sqrt{(\delta_1^2-4\delta_0\delta_2)\psi_2^2}}{\psi_2}$, we have the following explicit solitary wave solutions:

$$\begin{aligned}u_5(x,t)=\Bigg(\frac{1}{16}\Bigg(&\frac{4A^4\psi_2\operatorname{csc}h^4\left(\frac{A\xi}{2}\right)}{\left(A\cot h\left(\frac{A\xi}{2}\right)+\delta_1\right)^2}+\frac{8A^2(A\psi_2+\delta_1\psi_2)\operatorname{csc}h^2\left(\frac{A\xi}{2}\right)}{A\cot h\left(\frac{A\xi}{2}\right)+\delta_1}-\frac{8(A^2(-\delta_1)\psi_2^3+A^2\psi_2^2+2\delta_0\delta_2\psi_2^2)}{\psi_2}\\&-\psi_2\left(A\left(\tanh\left(\frac{A\xi}{4}\right)+\cot h\left(\frac{A\xi}{4}\right)\right)+2\delta_1\right)^2-4(A\psi_2-\delta_1\psi_2)\left(A\left(\tanh\left(\frac{A\xi}{4}\right)+\cot h\left(\frac{A\xi}{4}\right)\right)+2\delta_1\right),\end{aligned} \tag{24}$$

$$u_6(x,t)=\left(-\frac{\sec h^2\left(\frac{A\xi}{2}\right)(\psi_2(A^2\psi_2\sin h(A\xi)+A^2\psi_2)+A^2\psi_2^2(\cos h(A\xi)+1))}{4\psi_2}\right), \tag{25}$$

where $A=\sqrt{\delta_1^2-4\delta_2\delta_0}$.

When $a_0=\frac{k(-\delta_1\sqrt{(\delta_1^2-4\delta_0\delta_2)k^2}+\delta_1^2k-4\delta_0\delta_2k)}{\gamma_1\sqrt{(\delta_1^2-4\delta_0\delta_2)k^2}}$, $a_1=-\frac{2\delta_2k}{\gamma_1}$, $a_2=0$, $\psi_1=\frac{2k}{\gamma_1}$, $\psi_2=0$, $\nu=-\frac{k(\gamma_2+(\delta_1^2-4\delta_0\delta_2)k^2)}{\sqrt{(\delta_1^2-4\delta_0\delta_2)k^2}}$, $\gamma_3=\frac{\gamma_1\gamma_2}{2\sqrt{(\delta_1^2-4\delta_0\delta_2)k^2}}$, we have singular soliton solutions as follows:

$$u_7(x,t)=\left(\frac{\sqrt{(\delta_1^2-4\delta_0\delta_2)k^2}+\sqrt{\delta_1^2-4\delta_0\delta_2}k\cot h\left(\frac{1}{2}\sqrt{\delta_1^2-4\delta_0\delta_2}\xi\right)}{\gamma_1}\right), \tag{26}$$

$$u_8(x,t)=\left(\frac{\sqrt{(\delta_1^2-4\delta_0\delta_2)k^2}+\sqrt{\delta_1^2-4\delta_0\delta_2}k\left(1-\frac{2}{i\sin h\left(\sqrt{\delta_1^2-4\delta_0\delta_2}\xi\right)+i\cos h\left(\sqrt{\delta_1^2-4\delta_0\delta_2}\xi\right)+1}\right)}{\gamma_1}\right), \tag{27}$$

(II): When $\delta_1^2-4\delta_0\delta_2<0$, $\delta_1\delta_2\neq 0$, $\delta_0\delta_2\neq 0$, and $a_0=\frac{k(-\delta_1\sqrt{(\delta_1^2-4\delta_0\delta_2)k^2}+\delta_1^2k-4\delta_0\delta_2k)}{\gamma_1\sqrt{(\delta_1^2-4\delta_0\delta_2)k^2}}$, $a_1=-\frac{2\delta_2k}{\gamma_1}$, $a_2=0$, $\psi_1=\frac{2k}{\gamma_1}$, $\psi_2=0$, $\nu=-\frac{k(\gamma_2+(\delta_1^2-4\delta_0\delta_2)k^2)}{\sqrt{(\delta_1^2-4\delta_0\delta_2)k^2}}$, $\gamma_3=\frac{\gamma_1\gamma_2}{2\sqrt{(\delta_1^2-4\delta_0\delta_2)k^2}}$, implies the periodic solutions as follows:

$$u_9(x,t)=\left(\frac{B^2k\sec^2\left(\frac{B\xi}{2}\right)}{\gamma_1\left(B\tan\left(\frac{K\xi}{2}\right)-\delta_1\right)}-\frac{k\left(B\tan\left(\frac{K\xi}{2}\right)-\delta_1\right)}{\gamma_1}+\frac{k(\delta_1^2k-4\delta_0\delta_2k-\delta_1\mathrm{kB})}{\gamma_1\mathrm{kB}}\right), \tag{28}$$

$$u_{10}(x,t)=\left(-\frac{B^2k\csc^2\left(\frac{B\xi}{2}\right)}{\gamma_1\left(B\cot\left(\frac{B\xi}{2}\right)+\delta_1\right)}+\frac{k\left(B\cot\left(\frac{B\xi}{2}\right)+\delta_1\right)}{\gamma_1}+\frac{k(-\mathrm{Bk}\delta_1+\delta_1^2k-4\delta_0\delta_2k)}{\mathrm{Bk}\gamma_1}\right), \tag{29}$$

$$u_{11}(x,t)=\left(\frac{k\left(\frac{8\delta_0\delta_2-2\delta_1^2}{\delta_1(\sin(B\xi)-1)+B\cos(B\xi)}-B(\tan(B\xi)+\sec(B\xi))+\frac{\mathrm{kB}}{k}\right)}{\gamma_1}\right), \tag{30}$$

$$u_{12}(x,t)=\left(\frac{\delta_1\left(Bk\cot\left(\frac{B\xi}{2}\right)+\mathrm{kB}\right)+\mathrm{kB}^2\cot\left(\frac{B\xi}{2}\right)+\delta_1^2k-4\delta_0\delta_2k}{\gamma_1\left(B\cot\left(\frac{B\xi}{2}\right)+\delta_1\right)}\right). \tag{31}$$

When $a_0=-\frac{2\delta_0\delta_2\psi_2^2-\delta_1\psi_2\sqrt{(\delta_1^2-4\delta_0\delta_2)\psi_2^2}+\sqrt{(\delta_1^2-4\delta_0\delta_2)^2\psi_2^4}}{2\psi_2}$, $a_1=\delta_2(\sqrt{(\delta_1^2-4\delta_0\delta_2)\psi_2^2}-\delta_1\psi_2)$, $a_2=-\delta_2^2\psi_2$, $\psi_1=-\sqrt{(\delta_1^2-4\delta_0\delta_2)\psi_2^2}-\delta_1\psi_2$, $\gamma_2=-\frac{6k^2\sqrt{(\delta_1^2-4\delta_0\delta_2)^2\psi_2^4}}{\psi_2^2}$, $\gamma_3=\frac{6k^2}{\psi_2}$, $\gamma_1=0$, $\nu=\frac{5k^2\sqrt{(\delta_1^2-4\delta_0\delta_2)\psi_2^2}}{\psi_2}$, we have the following periodic solutions:

$$\begin{aligned}u_{13}(x,t)=&\frac{1}{16}\left(4(\mathrm{B}\psi_2-\delta_1\psi_2)\left(B\left(\tan\left(\frac{B\xi}{4}\right)-\cot\left(\frac{B\xi}{4}\right)\right)-2\delta_1\right)-\psi_2\left(B\left(\tan\left(\frac{B\xi}{4}\right)-\cot\left(\frac{B\xi}{4}\right)\right)-2\delta_1\right)^2\right.\\&\left.+\frac{4B^4\psi_2\csc^4\left(\frac{B\xi}{2}\right)}{\left(B\cot\left(\frac{B\xi}{2}\right)+\delta_1\right)^2}-\frac{8B^2\csc^2\left(\frac{B\xi}{2}\right)(\mathrm{B}\psi_2+\delta_1\psi_2)}{B\cot\left(\frac{B\xi}{2}\right)+\delta_1}-\frac{8(-\mathrm{B}\psi_2\delta_1\psi_2+\mathrm{B}\psi_2^2+2\delta_0\delta_2\psi_2^2)}{\psi_2},\right.\end{aligned} \tag{32}$$

$$u_{14}(x,t)=\left(-\frac{\sec^2\left(\frac{B\xi}{2}\right)(\psi_2(B^2\psi_2-B^2\psi_2\sin(B\xi))+B^2\psi_2^2(\cos(B\xi)+1))}{4\psi_2}\right), \tag{33}$$

$$u_{15}(x,t)=\left(-\frac{\csc^2\left(\frac{B\xi}{2}\right)(\psi_2(B^2\psi_2\sin(B\xi)+B^2\psi_2)-B^2\psi_2^2(\cos(B\xi)-1))}{4\psi_2}\right), \tag{34}$$

Where $B=\sqrt{4\delta_0\delta_2-\delta_1^2}$. When $a_0=\frac{\gamma_2\left(\frac{\gamma_3\delta_1}{\sqrt{\gamma_3^2(\delta_1^2-4\delta_0\delta_2)}}+1\right)}{2\gamma_3}$, $a_1=\frac{\gamma_2\delta_2}{\sqrt{\gamma_3^2(\delta_1^2-4\delta_0\delta_2)}}$, $\psi_1=0$, $\psi_2=0$, $a_2=0$, $k=-\frac{\gamma_1\gamma_2}{2\sqrt{\gamma_3^2(\delta_1^2-4\delta_0\delta_2)}}$, $\nu=\frac{\gamma_2(\gamma_2\gamma_1^2+4\gamma_3^2)}{4\gamma_3\sqrt{\gamma_3^2(\delta_1^2-4\delta_0\delta_2)}}$, we have the following solutions:

$$u_{16}(x,t)=\left(\frac{1}{2}\gamma_2\left(\frac{\delta_1-\frac{4\delta_0\delta_2\cos\left(\sqrt{4\delta_0\delta_2-\delta_1^2}\xi\right)}{\sqrt{4\delta_0\delta_2-\delta_1^2}\left(\sin\left(\sqrt{4\delta_0\delta_2-\delta_1^2}\xi\right)+1\right)+\delta_1\cos\left(\sqrt{4\delta_0\delta_2-\delta_1^2}\xi\right)}}{\sqrt{\gamma_3^2(\delta_1^2-4\delta_0\delta_2)}}+\frac{1}{\gamma_3}\right)\right), \tag{35}$$

$$u_{17}(x,t)=\frac{1}{2}\gamma_2\left(\frac{\delta_1-\frac{4\delta_0\delta_2\sin\left(\sqrt{4\delta_0\delta_2-\delta_1^2}\xi\right)}{\delta_1\sin\left(\sqrt{4\delta_0\delta_2-\delta_1^2}\xi\right)-\sqrt{4\delta_0\delta_2-\delta_1^2}\left(\cos\left(\sqrt{4\delta_0\delta_2-\delta_1^2}\xi\right)+1\right)}}{\sqrt{\gamma_3^2(\delta_1^2-4\delta_0\delta_2)}}+\frac{1}{\gamma_3}\right), \tag{36}$$

where $\xi=\frac{k}{\beta}(x+\frac{1}{\Gamma(\beta)})^\beta-\frac{\nu}{\beta}(t+\frac{1}{\Gamma(\beta)})^\beta$.

(III) When $a_0=\frac{\gamma_2\left(\frac{\gamma_3\delta_1}{\sqrt{\gamma_3^2(\delta_1^2-4\delta_0\delta_2)}}+1\right)}{2\gamma_3}$, $a_1=\frac{\gamma_2\delta_2}{\sqrt{\gamma_3^2(\delta_1^2-4\delta_0\delta_2)}}$, $\psi_1=0$, $\psi_2=0$, $a_2=0$, $k=-\frac{\gamma_1\gamma_2}{2\sqrt{\gamma_3^2(\delta_1^2-4\delta_0\delta_2)}}$, $\nu=\frac{\gamma_2(\gamma_2\gamma_1^2+4\gamma_3^2)}{4\gamma_3\sqrt{\gamma_3^2(\delta_1^2-4\delta_0\delta_2)}}$, $\delta_0=0$, we have the solitary wave solutions as follows:

$$u_{18}(x,t)=\left(\frac{\gamma_2\left(\frac{\gamma_3\delta_1}{\sqrt{\gamma_3^2\delta_1^2}}+1\right)}{2\gamma_3}-\frac{\gamma_2\delta_1\rho}{\sqrt{\gamma_3^2\delta_1^2}(-\sin h(\delta_1\xi)+\cos h(\delta_1\xi)+\rho)}\right), \tag{37}$$

$$u_{19}(x,t)=\left(\frac{\gamma_2\left(\frac{\gamma_3\delta_1}{\sqrt{\gamma_3^2\delta_1^2}}+1\right)}{2\gamma_3}-\frac{\gamma_2\delta_1(\sin h(\delta_1\xi)+\cos h(\delta_1\xi))}{\sqrt{\gamma_3^2\delta_1^2}(\sin h(\delta_1\xi)+\cos h(\delta_1\xi)+\rho)}\right), \tag{38}$$

where ρ represents a constant and ξ given in Equation (6).

5. Graphical View and Discussion

The current section uses Mathematica as a computational tool to study the graphical characteristics of the soliton in the proposed model traveling wave solutions. Different visual representations of 3D graphical representations reveal the evolution of wave propagation over time at many parameter settings. By use of several graph forms, one may see the characteristics and behavior of the waves. Moreover, the use of a thorough representation of wave dynamics, 3D charts with color coding, may efficiently show the relationship between spatial and temporal components. A variety of solitary waves have been sketched in Figures 1–4 together with the effect of fractional parameters.

The comprehension of cardiovascular health and disease is significantly influenced by the presence of solitary waves in blood vessel dynamics. These nonlinear, localize waves propagate through arterial walls, preserving their shape and speed, thereby enabling more precise modeling of blood flow and pressure fluctuations than conventional linear methods. Insights into the effects of conditions such as hypertension and atherosclerosis, pulse propagation, and arterial rigidity are obtained through the study of solitary waves. Their capacity to travel long distances without dissipation renders them advantageous for the simulation of hydrodynamic behavior in large arteries. Furthermore, such waves facilitate the development of diagnostic instruments and therapeutic strategies, including the optimization of stent designs and the prediction

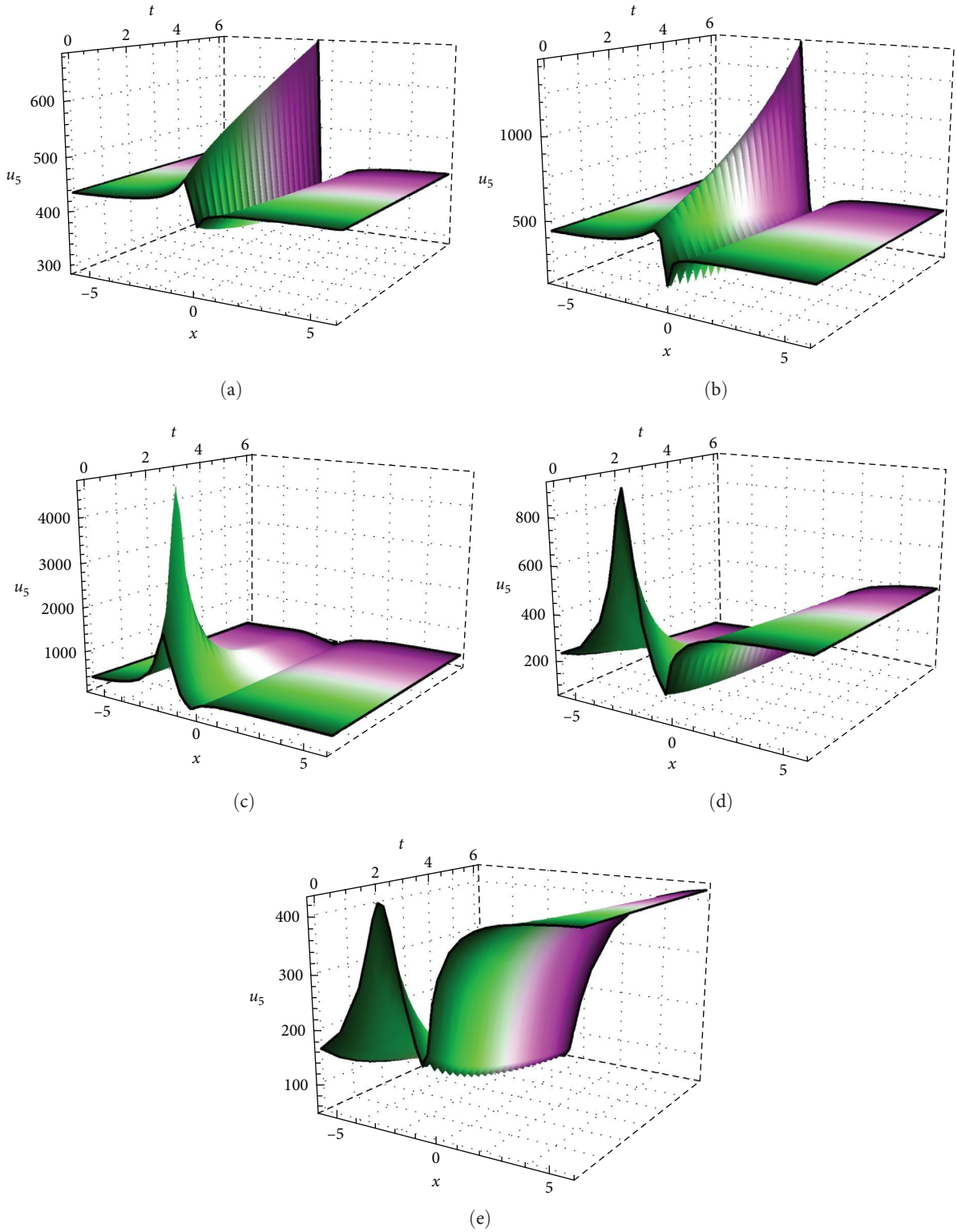

FIGURE 1: Graphs for Equation (16) with different values. (a) $\beta = 0.119$, (b) $\beta = 0.26$, (c) $\beta = 0.399$, (d) $\beta = 0.475$, and (e) $\beta = 0.51$.

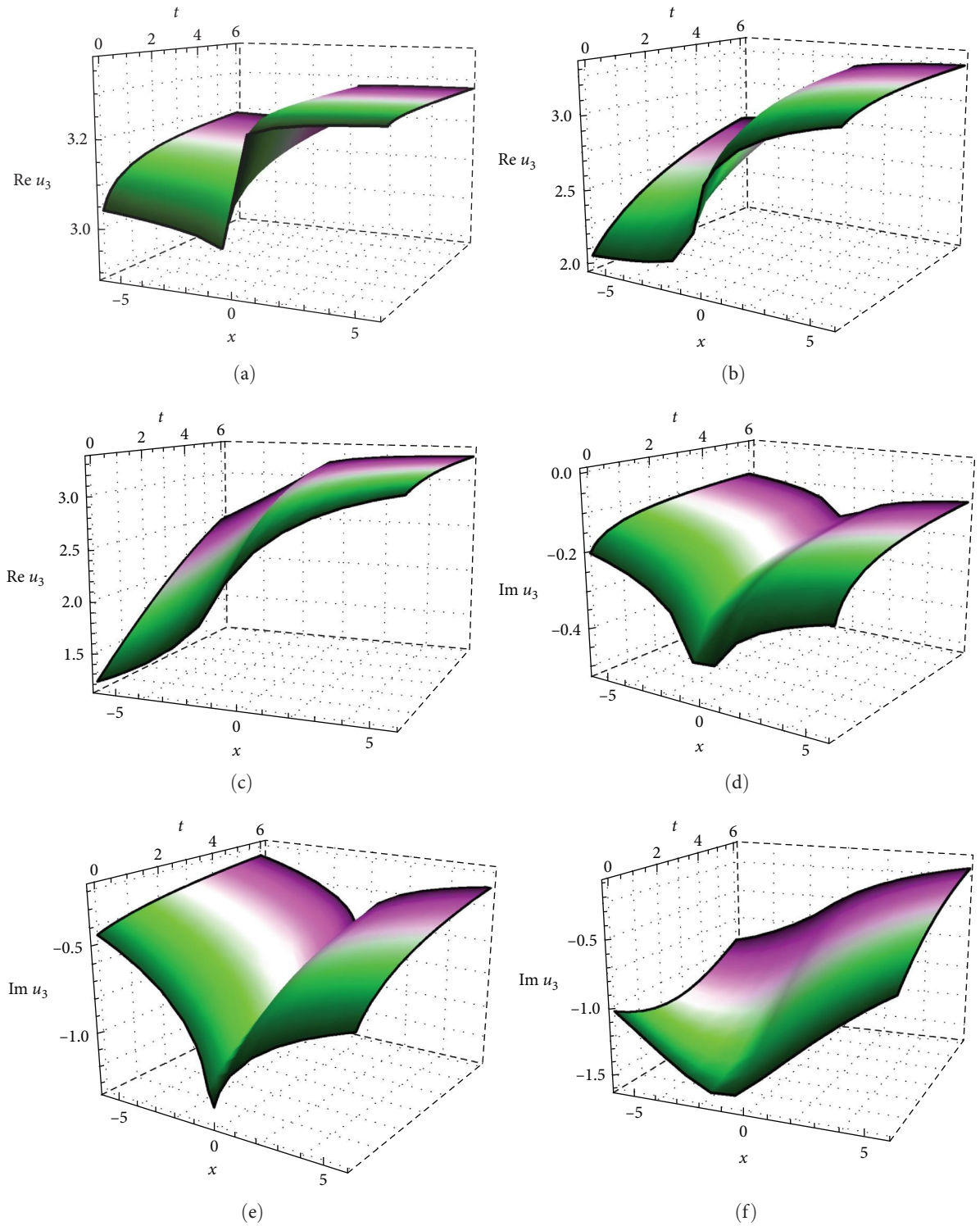

FIGURE 2: Graphs for Equation (22) with different values. (a) $\beta = 0.19$, (b) $\beta = 0.49$, (c) $\beta = 0.79$, (d) $\beta = 0.199$, (e) $\beta = 0.39$, and (f) $\beta = 0.89$.

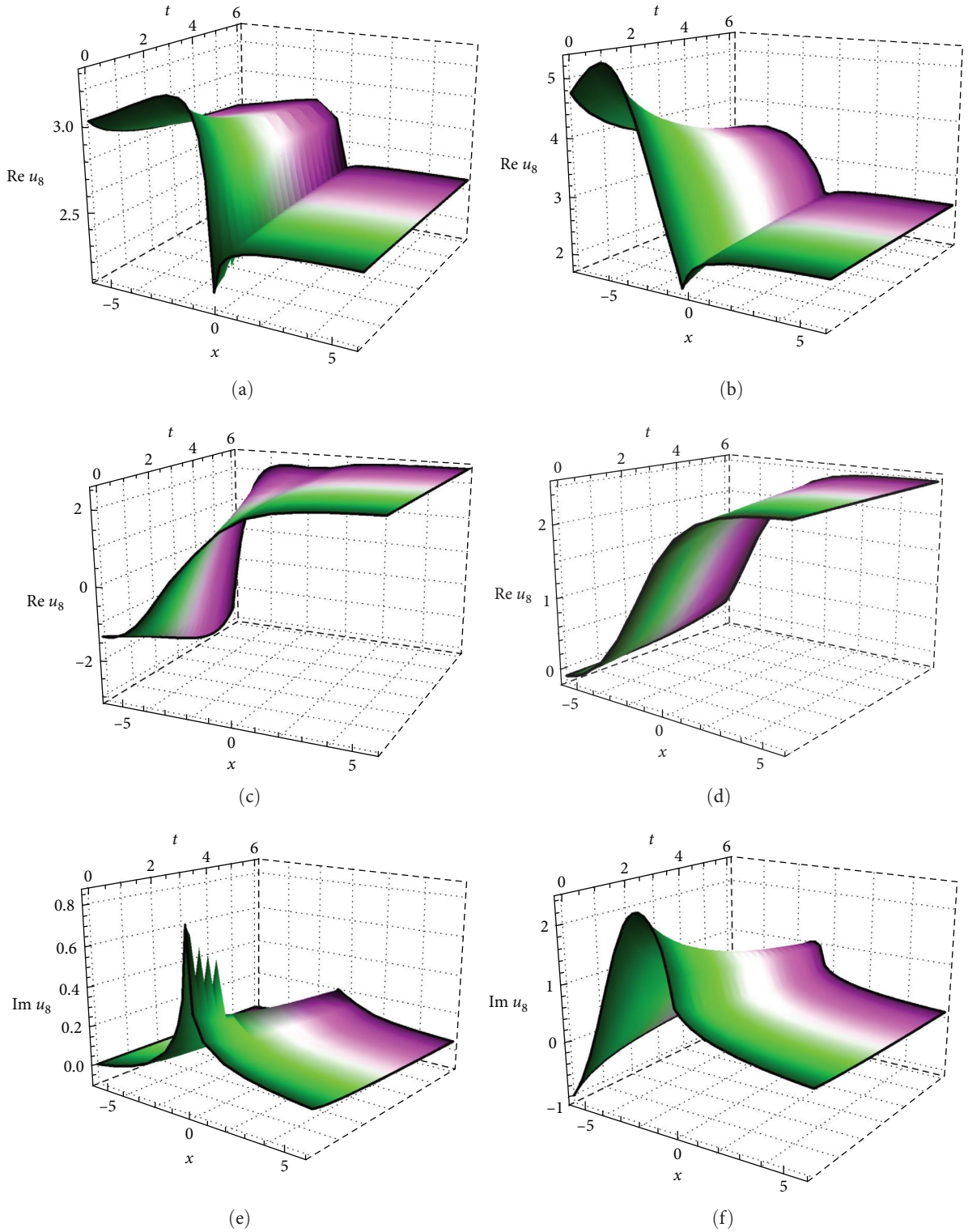

FIGURE 3: Continued.

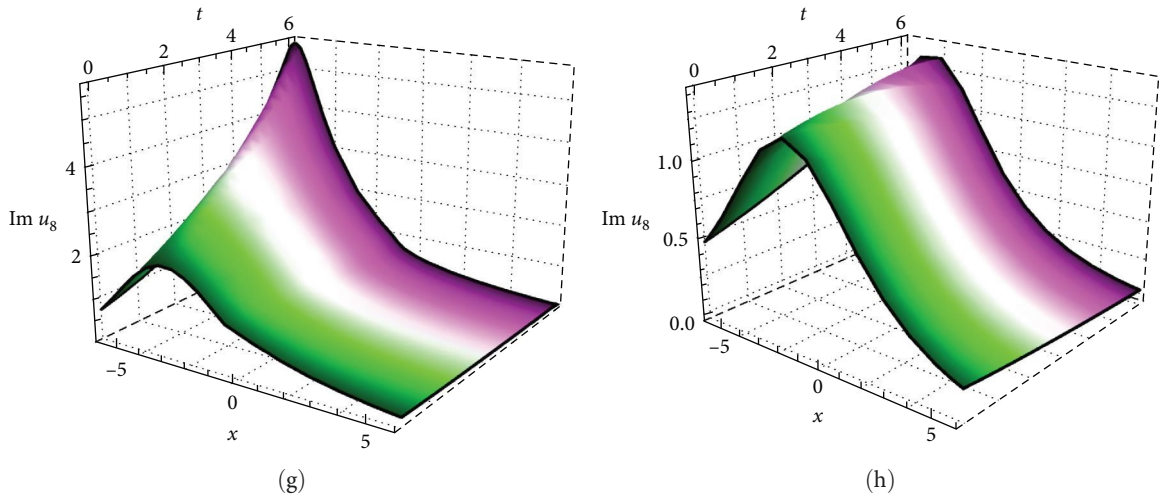

FIGURE 3: Graphs for Equation (27) with different values. (a) $\beta = 0.29$, (b) $\beta = 0.429$, (c) $\beta = 0.729$, (d) $\beta = 0.92$, (e) $\beta = 0.215$, (f) $\beta = 0.435$, (g) $\beta = 0.735$, and (h) $\beta = 0.976$.

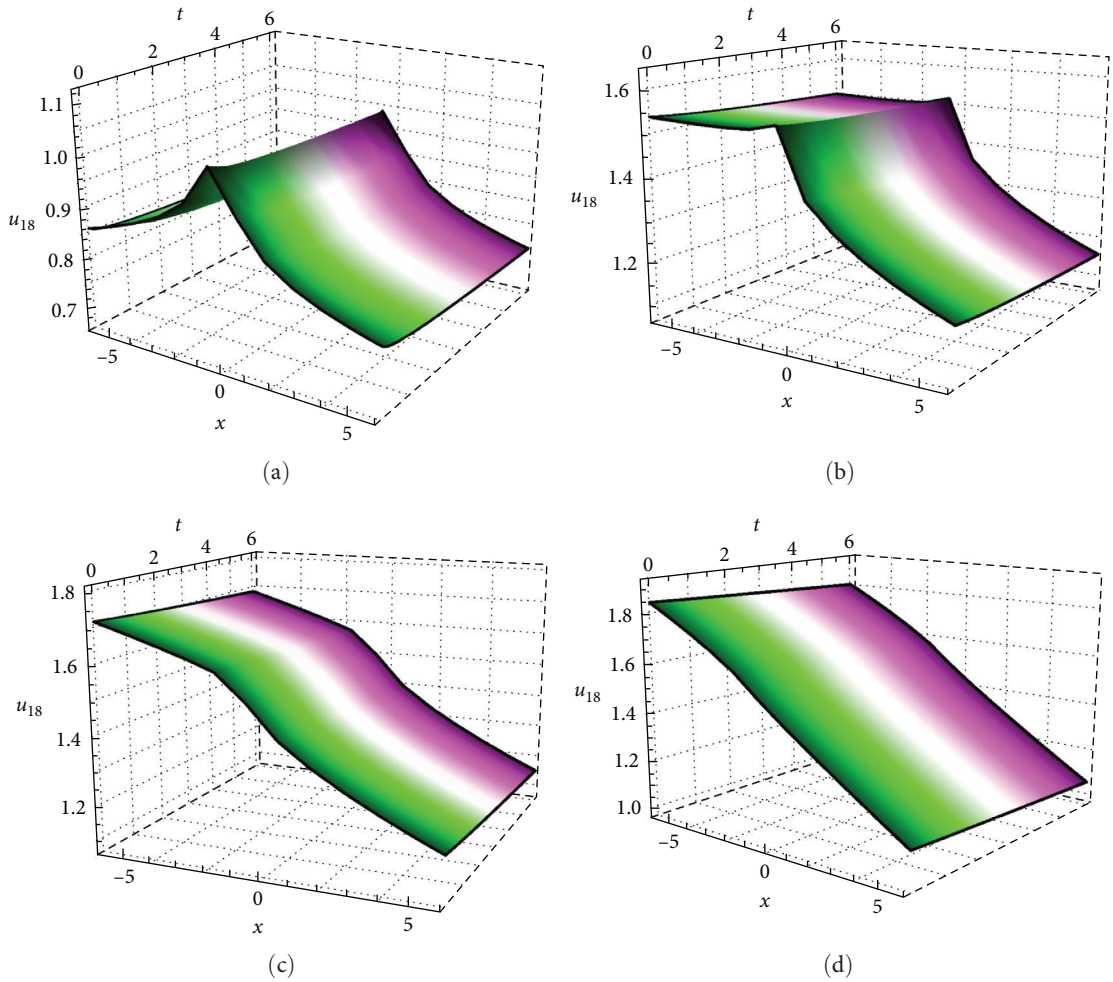

FIGURE 4: Graphs for Equation (37) with different values. (a) $\beta = 0.119$, (b) $\beta = 0.419$, (c) $\beta = 0.619$, and (d) $\beta = 0.899$.

of aneurysm rupture. Solitary wave models improve clinical interventions and increase our understanding of vascular mechanics by capturing the nonlinear elasticity of blood vessels.

6. Chaotic Analysis of Governing Equation With Perturbation Term

The chaotic behavior of the governing equation is discussed. The chaotic behavior in dynamical systems is crucial for understanding and modeling complex, nonlinear phenomena across many scientific and engineering disciplines. This behavior helps explain unpredictability in systems that are otherwise governed by deterministic laws. Let $\Phi' = G$ and planar dynamical system Equation (7), with perturbation term, can be expressed as follows:

$$\begin{aligned}\frac{d\Phi}{d\xi} &= G,\\ \frac{dG}{d\xi} &= -\frac{G(\xi)(\gamma_1\kappa\Phi(\xi)+\nu)}{k^2}+\frac{\gamma_3}{k^2}\Phi(\xi)^2-\frac{\gamma_2}{k^2}\Phi(\xi)+\Omega(\xi),\end{aligned} \tag{39}$$

where $\Omega = \alpha\cos\omega t$ is a perturbation term, and represents the outward periodic force, α and ω depict the frequency and intensity of the periodic phrase, respectively. The chaotic analysis is of significant biological importance, as it encapsulates the inherent nonlinearity and sensitivity of dynamic systems in living organisms. Chaos theory is an essential instrument for comprehending emergent patterns, bifurcations, and stability in biological contexts such as neural activity, cardiac rhythms, or biochemical reactions, where small perturbations can result in complex, unpredictable behaviors. Researchers can identify critical thresholds, early warning signals for disease, and resilience mechanisms by examining chaotic dynamics in systems such as blood flow, hormone regulation, or gene networks. External influences, such as stress, medications, or environmental changes, are accounted for by perturbation terms, which demonstrate the process by which biological systems transition from order to disorder. This method improves predictive modeling in medicine, allowing for the development of more effective strategies for the management of arrhythmia, neurological disorders, and the optimization of drug delivery systems, all of which are significantly influenced by the initial conditions. In our research, we observed chaotic behavior in system (39), characterized by unpredictable, time-dependent trajectories diverging from regular patterns. To detect chaos, we employed a 2D phase portrait and time series analysis. By giving the values of the suitable parameters, two-dimensional and time series analysis of the dynamical system (39) are shown in Figures 5 and 6.

7. Sensitivity Analysis

The present section examines the sensitivity analysis of Equation (7). Taking $\phi' = G$ and employing the Galilean transformation, Equation (7) is described such as [40, 41]:

$$\begin{aligned}\frac{d\Phi}{d\xi} &= G,\\ \frac{dG}{d\xi} &= -\frac{G(\xi)(\gamma_1\kappa\Phi(\xi)+\nu)}{k^2}+\frac{\gamma_3}{k^2}\phi(\xi)^2-\frac{\gamma_2}{k^2}\Phi(\xi).\end{aligned} \tag{40}$$

The objective of sensitivity analysis is to comprehend the impact of fluctuations in input parameters on the solution's behavior to the PDE. Sensitivity analysis in the context of NLPDEs involves examining how the solution of the PDE and its related values respond to variations in parameters as well as initial conditions.

The sensitivity of our system was assessed in this section by examining a variety of initial conditions, as illustrated in the accompanying Figures 7–10 by choosing the relevant parameter values $\gamma_1 = 0.1, \gamma_2 = 0.2, \gamma_3 = -0.1, k = -1.5, \nu = 1.8$. In Figure 7 red and green lines with initial condition $(\Phi, G) = (2.5, 0.5)$ and $(\Phi, G) = (2.8, 1)$ illustrates two distinct solutions. In Figure 8 $(\Phi, G) = (2.5, 0.5)$ in red and $(\Phi, G) = (3, 1.5)$ in magenta line represent the solution. In Figure 9, initial condition $(\Phi, G) = (2.8, 1)$ in green and $(\Phi, G) = (3, 1.5)$ in magenta depict the behaviors of two different types of solutions. Finally, the combination of all solutions is verified in one Figure 10 applying the initial conditions $(\Phi, G) = (2.5, 0.5)$ in red, $(\Phi, G) = (2.8, 1)$ in green and $(\Phi, G) = (3, 1.5)$ in magenta.

It has been demonstrated that the solution is not substantially affected by minor modifications to the initial values. Subsequently, the model in concern is not highly sensitive.

8. Conclusions

In this study, the dynamical behavior of the nonlinear Murray equation has been successfully investigated by using integration methods, namely the generalized Arnous method and the MGREMM. Our study demonstrates various solitary wave solutions in fractional forms and establishes the necessary conditions for the existence of these solutions, taking into account important physical factors. Through the application of the β-derivative and suitable wave transformations, a wide variety of solitary wave solutions, including mixed, singular, dark, bright, and combined solitons-have been successfully derived. The incorporation of graphical simulations for different parameter values has further illuminated the rich dynamical behaviors of the system. It is believed that the constraints imposed on the parameters ensure the formation of the obtained solitons. Our proposed approaches have yielded a series of solutions that contribute to the understanding of the specific physical phenomena of the proposed model. Mathematicians and other scientists are extremely intrigued by solitary wave solutions, as they offer a fundamental explanation of nonlinear phenomena that have numerous practical applications.

Additionally, the system's chaotic and sensitivity analysis to initial conditions has also been explored. The methods presented here may be used in a wide variety of fields, including oceanography, differential geometry of curves, plasma physics, optical communications, and many nonlinear systems in

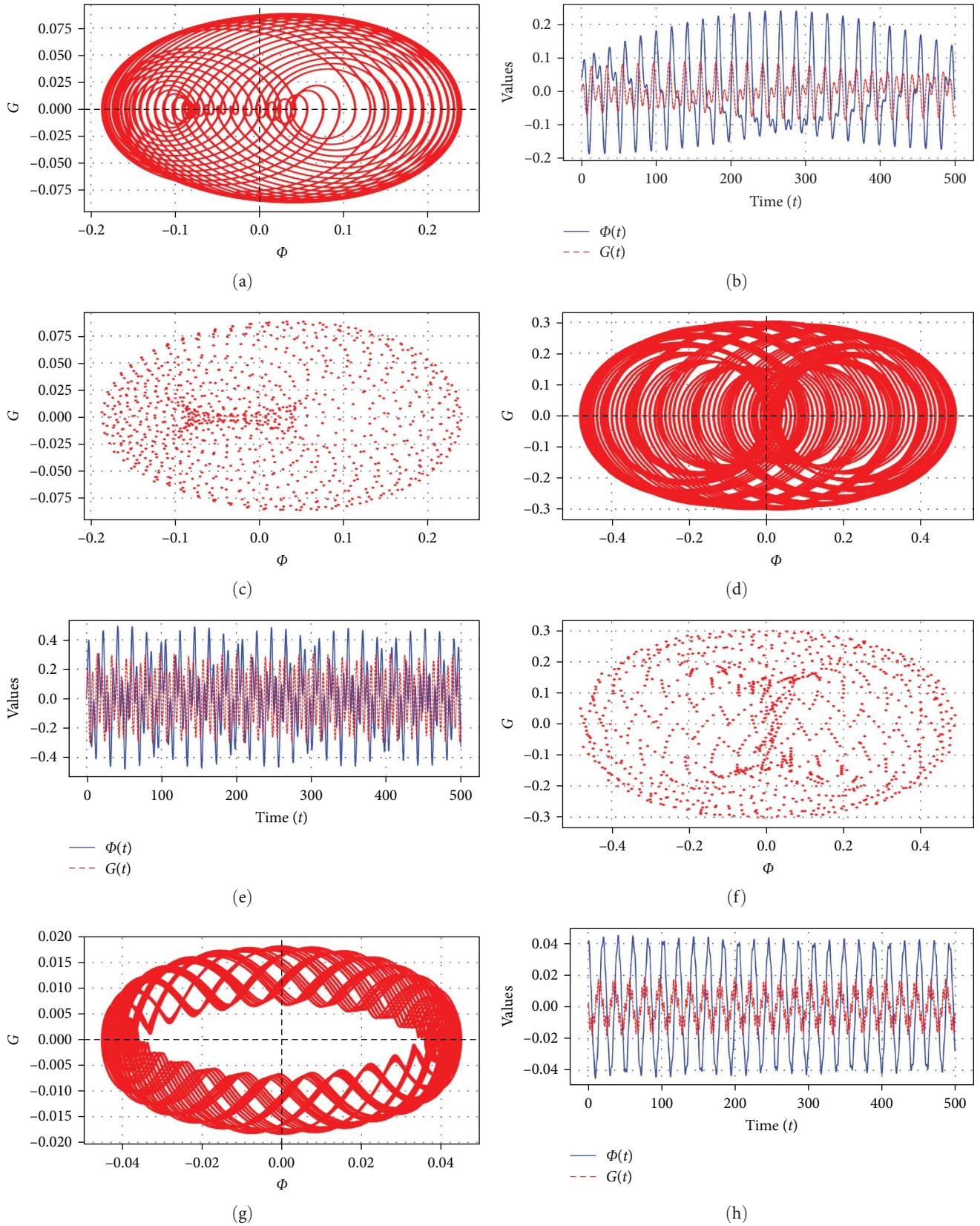

Figure 5: Continued.

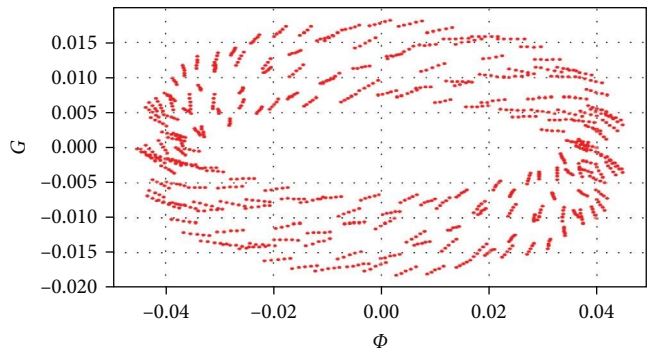

(i)

FIGURE 5: Plots for chaos in system (39) using 2D phase portrait, time analysis and Poincaré maps with $\gamma_1 = 0.01$, $k = 4.5$, $\nu = 0.008$, $\gamma_2 = 1.9$, $\gamma_3 = 0.4$, and taking the initial conditions $(0, 0.04)$. (a) $\alpha = 0.02$, $\omega = 0.60$, (b) $\alpha = 0.02$, $\omega = 0.60$, (c) $\alpha = 0.02$, $\omega = 0.60$, (d) $\alpha = 0.2$, $\omega = 0.98$, (e) $\alpha = 0.2$, $\omega = 0.99$, (f) $\alpha = 0.2$, $\omega = 0.98$, (g) $\alpha = 0.01$, $\omega = 1.9$, (h) $\alpha = 0.01$, $\omega = 1.9$, and (i) $\alpha = 0.01$, $\omega = 1.9$.

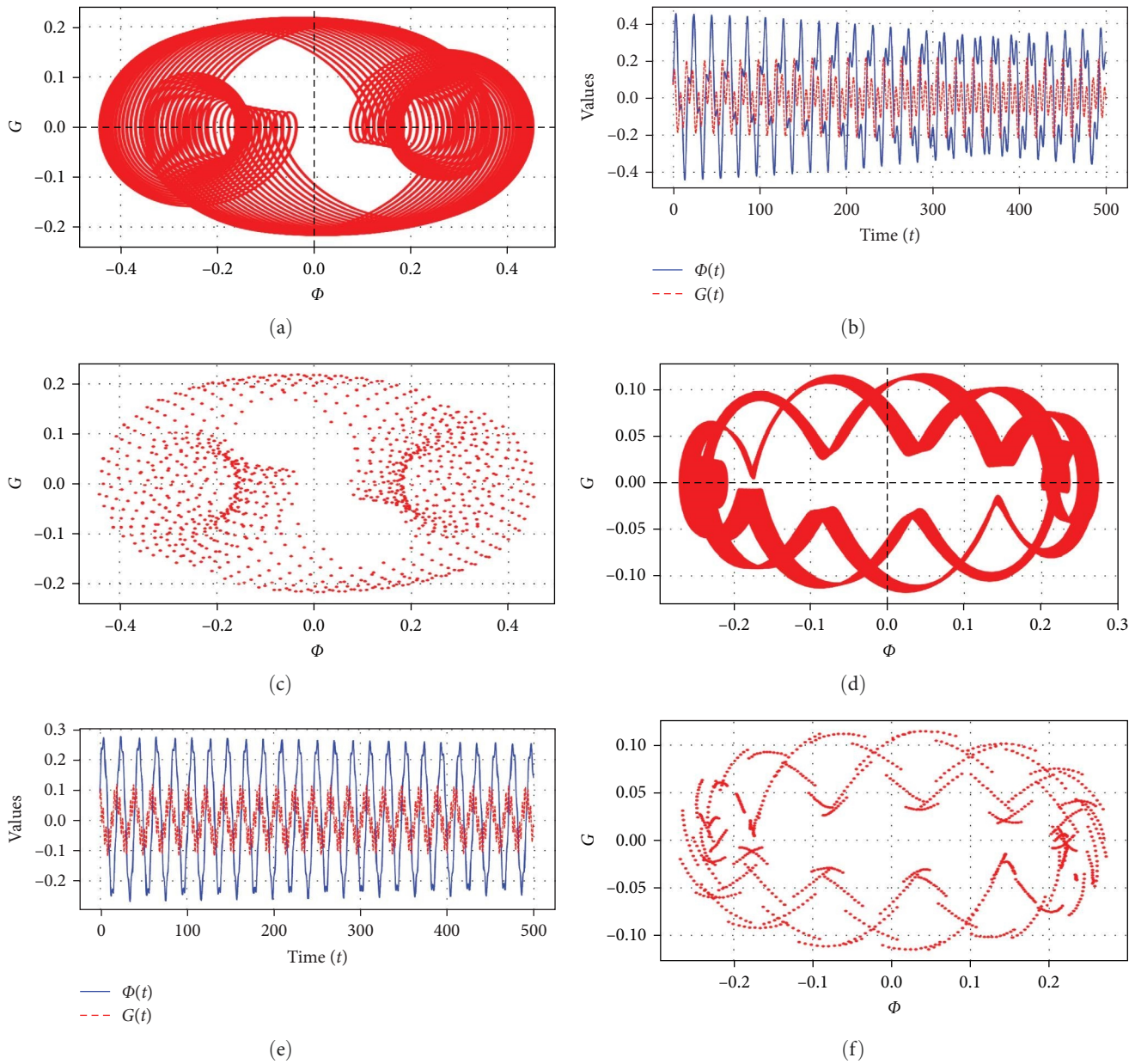

FIGURE 6: Continued.

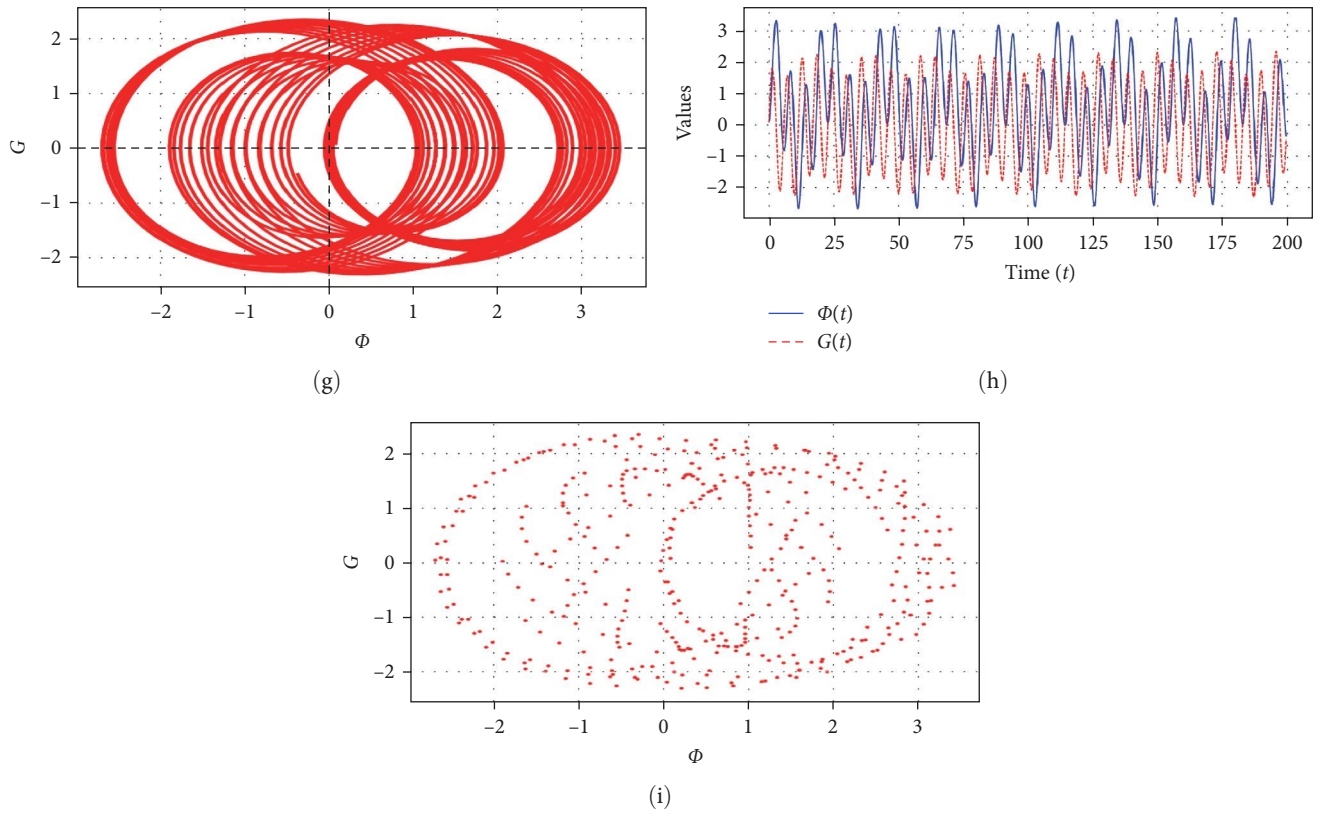

FIGURE 6: Plots for chaos in system (39) using 2D phase portrait, time analysis and Poincaré maps with $\gamma_1 = 0.01, k = 4.5, \nu = 0.008, \gamma = 1.9, \gamma_3 = 0.4$, and taking the initial conditions $(0.7, 0.09)$. (a) $\alpha = 0.1, \omega = 0.91$, (b) $\alpha = 0.1, \omega = 0.91$, (c) $\alpha = 0.1, \omega = 0.91$, (d) $\alpha = 0.08, \omega = 1.99$, (e) $\alpha = 0.08, \omega = 1.99$, (f) $\alpha = 0.08, \omega = 1.99$, (g) $\alpha = 1.99, \omega = 1.098$, (h) $\alpha = 1.99, \omega = 1.098$, and (i) $\alpha = 1.99, \omega = 1.098$.

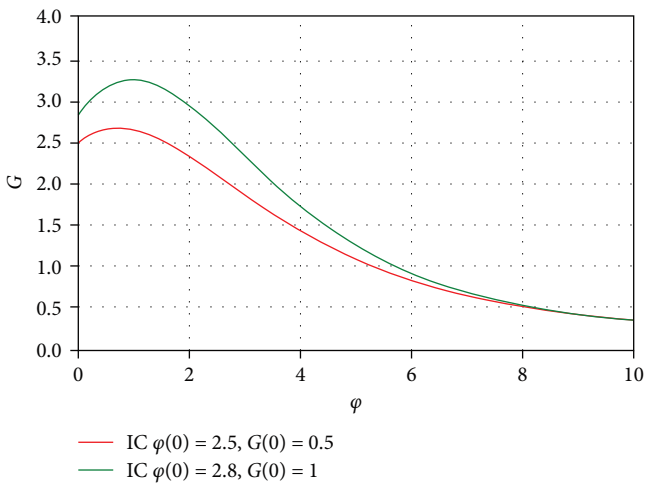

FIGURE 7: Plot for the system (40).

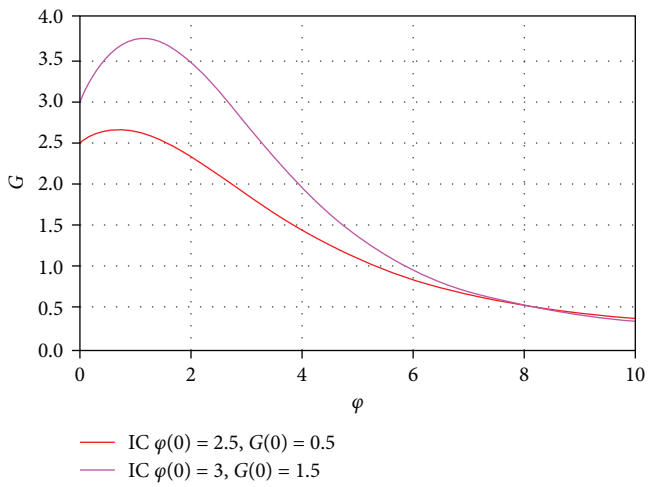

FIGURE 8: Plot for the system (40).

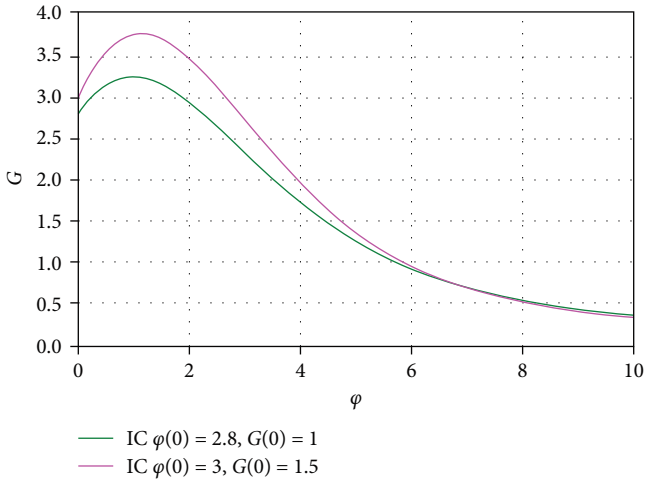

FIGURE 9: Plot for the system (40).

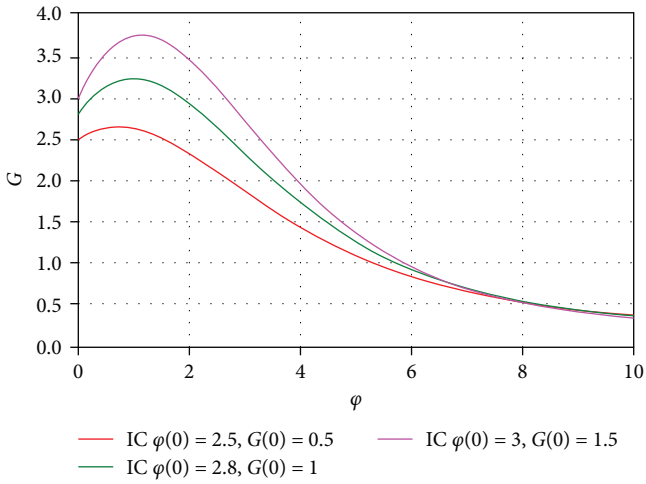

FIGURE 10: Plot for the system (40).

biological phenomena. This study demonstrates the efficacy of the integration techniques employed in the analysis of a variety of NLEEs and FNLPDEs that are frequently encountered in nonlinear science. In conclusion, this study offers novel insights into the dynamics of solitary waves in nonlinear systems with fractional dynamics, marking a significant contribution to the analytical treatment of reaction-diffusion equations and paving the way for further research and practical applications in complex biological and physical modeling.

Data Availability Statement

No data were generated for this study.

Conflicts of Interest

The authors declare no conflicts of interest.

Funding

No funding was received for this manuscript.

References

[1] J. D. Murray, *Nonlinear Differential Equation Models in Biology* (Clarendon Press, 1977).
[2] L. Ming, J. Muhammad, D. Yaro, and U. Younas, "Exploring the Multistability, Sensitivity, and Wave Profiles to the Fractional Sharma–Tasso–Olver Equation in the Mathematical Physics," *AIP Advances* 15, no. 4 (2025).
[3] J. Muhammad, U. Younas, H. Rezazadeh, M. A. Hosseinzadeh, and S. Salahshour, "On the Investigation of Fractional Coupled Nonlinear Integrable Dynamical System: Dynamics of Soliton Solutions," *Modern Physics Letters B* 38, no. 36 (2024): 2450380.
[4] Q. Hou, Y. Li, V. P. Singh, and Z. Sun, "Physics-Informed Neural Network for Diffusive Wave Model," *Journal of Hydrology* 637 (2024): 131261.
[5] S. Manukure and T. Booker, "A Short Overview of Solitons and Applications," *Partial Differential Equations in Applied Mathematics* 4 (2021): 100140.
[6] J. Muhammad, M. B. Riaz, U. Younas, N. Nasreen, A. Jhangeer, and D. Lu, "Extraction of Optical Wave Structures to the Coupled Fractional System in Magneto-Optic Waveguides," *Arab Journal of Basic and Applied Sciences* 31, no. 1 (2024): 242–254.
[7] U. Younas, J. Ren, T. A. Sulaiman, M. Bilal, and A. Yusuf, "On the Lump Solutions, Breather Waves, Two-Wave Solutions of (2+1)-Dimensional Pavlov Equation and Stability Analysis," *Modern Physics Letters B* 36, no. 14 (2022): 2250084.
[8] P. Wan, J. Manafian, H. F. Ismael, and S. A. Mohammed, "Investigating One-, Two-, and Triple-Wave Solutions via Multiple Exp-Function Method Arising in Engineering Sciences," *Advances in Mathematical Physics* 2020 (2020): 8018064, 18.
[9] B. Li and F. Wang, "New Solutions to a Category of Nonlinear PDEs," *Frontiers in Physics* 13 (2025): 1547245.
[10] B. Li, F. Wang, and S. Nadeem, "Explicit and Exact Travelling Wave Solutions for Hirota Equation and Computerized Mechanization," *PLoS ONE* 19, no. 5 (2024): e0303982.
[11] S.-D. Zhu, "The Generalizing Riccati Equation Mapping Method in Non-Linear Evolution Equation: Application to (2 + 1)-Dimensional Boiti-Leon-Pempinelle Equation," *Chaos, Soliton and Fractals* 37, no. 5 (2008): 1335–1342.
[12] J. S. Duan, R. Rach, D. Baleanu, and A. M. Wazwaz, "A Review of the Adomian Decomposition Method and Its Applications to Fractional Differential Equations," *Communications in Fractional Calculus* 3, no. 2 (2012): 73–99.
[13] M. Mañas, "Darboux Transformations for the Nonlinear Schrödinger Equations," *Journal of Physics A: Mathematical and General* 29, no. 23 (1996): 7721–7737.
[14] K. Hosseini, F. Samadani, D. Kumar, and M. Faridi, "New Optical Solitons of Cubic-Quartic Nonlinear Schrödinger Equation," *Optik* 157 (2018): 1101–1105.
[15] T. Han, Z. Li, and C. Li, "Bifurcation Analysis, Stationary Optical Solitons and Exact Solutions for Generalized Nonlinear Schrödinger Equation With Nonlinear Chromatic Dispersion and Quintuple Power-Law of Refractive Index in Optical Fibers," *Physica A: Statistical Mechanics and its Applications* 615 (2023): 128599.
[16] Y. Gu, B. Chen, F. Ye, and N. Aminakbari, "Soliton Solutions of Nonlinear Schrödinger Equation With the Variable Coefficients Under the Influence of Woods–Saxon Potential," *Results in Physics* 42 (2022): 105979.
[17] E. A. Az-Zo'bi, "New Kink Solutions for the Van der Waals p-System," *Mathematical Methods in the Applied Sciences* 42, no. 18 (2019): 6216–6226.

[18] N. A. Shah, P. Agarwal, J. D. Chung, E. R. El-Zahar, and Y. S. Hamed, "Analysis of Optical Solitons for Nonlinear Schrödinger Equation With Detuning Term by Iterative Transform Method," *Symmetry* 12, no. 11 (2020): 1850.
[19] J. Muhammad, Q. Ali, and U. Younas, "Three Component Coupled Fractional Nonlinear Schrodinger Equations: Diversity of Exact Optical Solitonic Structures," *Modern Physics Letters B* 38, no. 36 (2024): 2450373.
[20] A. Batool, N. Raza, J. F. Gómez-Aguilar, and V. H. Olivares-Peregrino, "Extraction of Solitons From Nonlinear Refractive Index Cubic-Quartic Model via a Couple of Integration Norms," *Optical and Quantum Electronics* 54, no. 9 (2022): 549.
[21] C. Chen and Y.-L. Jiang, "Simplest Equation Method for Some Time-Fractional Partial Differential Equations With Conformable Derivative," *Computers & Mathematics with Applications* 75, no. 8 (2018): 2978–2988.
[22] J. Muhammad, G. H. Tipu, and U. Younas, "Analytical Solutions of the Eighth-Order (3+1)-Dimensional Kac-Wakimoto Equation Modeling Waves in Ocean Engineering," *Modeling Earth Systems and Environment* 11 (2025): 381.
[23] J. Shi, C. Liu, and J. Liu, "Hypergraph-Based Model for Modeling Multi-Agent Q-Learning Dynamics in Public Goods Games," *IEEE Transactions on Network Science and Engineering* 11, no. 6 (2024): 6169–6179.
[24] K. Luo, Q. Fu, X. Liu, et al., "Study of Polarization Transmission Characteristics in Nonspherical Media," *Optics and Lasers in Engineering* 174 (2024): 107970.
[25] U. Younas, J. Muhammad, and E. Hussain, "Higher Dimensional Nonlinear Model Arising to the Diversity of Fields: Dynamics of Wave Structures With M-Fractional Derivative," *Partial Differential Equations in Applied Mathematics* 16 (2025): 101284.
[26] X. Chen and R. Jing, "Video Super Resolution Based on Deformable 3D Convolutional Group Fusion," *Scientific Reports* 15, no. 1 (2025): 9050.
[27] A. Jhangeer, W. A. Faridi, and M. Alshehri, "The Study of Phase Portraits, Multistability Visualization, Lyapunov Exponents and Chaos Identification of Coupled Nonlinear Volatility and Option Pricing Model," *The European Physical Journal Plus* 139, no. 7 (2024): 658.
[28] A. Q. Khan, T. Akhtar, A. Jhangeer, and M. B. Riaz, "Codimension-Two Bifurcation Analysis at an Endemic Equilibrium State of a Discrete Epidemic Model," *AIMS Mathematics* 9, no. 5 (2024): 13006–13027.
[29] A. Jhangeer and Beenish, "Ferroelectric Frontiers: Navigating Phase Portraits, Chaos, Multistability and Sensitivity in Thin-Film Dynamics," *Chaos, Solitons & Fractals* 188 (2024): 115540.
[30] A. Jhangeer, F. Ibraheem, T. Jamal, A. Abdul Rahimzai, and I. Khan, "Investigating Pseudo Parabolic Dynamics Through Phase Portraits, Sensitivity, Chaos and Soliton Behavior," *Scientific Reports* 14, no. 1 (2024): 15224.
[31] A. H. Arnous, "Optical Solitons to the Cubic Quartic Bragg Gratings With Anti-Cubic Nonlinearity Using New Approach," *Optik* 251 (2022): 168356.
[32] S. Kumar, I. Hamid, and M. A. Abdou, "Dynamic Frameworks of Optical Soliton Solutions and Soliton-Like Formations to Schrödinger–Hirota Equation With Parabolic Law Non-Linearity Using a Highly Efficient Approach," *Optical and Quantum Electronics* 55, no. 14 (2023): 1261.
[33] M. A. Al Zubi, K. Afef, and E. A. Az-Zo'bi, "Assorted Spatial Optical Dynamics of a Generalized Fractional Quadruple Nematic Liquid Crystal System in Non-Local Media," *Symmetry* 16, no. 6 (2024): 778.
[34] E. Az-Zo'bi, L. Akinyemi, and A. O. Alleddawi, "Construction of Optical Solitons for Conformable Generalized Model in Nonlinear Media," *Modern Physics Letters B* 35, no. 24 (2021): 2150409.
[35] A. Atangana, D. Baleanu, and A. Alsaedi, "Analysis of Time-Fractional Hunter-Saxton Equation: A Model of Neumatic Liquid Crystal," *Open Physics* 14, no. 1 (2016): 145–149.
[36] E. S. Al-Rawi and A. F. Qasem, "Numerical Solution for Nonlinear Murray Equation Using the Operational Matrices of the Haar Wavelets Method," *Tikrit Journal of Pure Science* 15, no. 2 (2010): 288–294.
[37] R. M. Cherniha, "New Ansätze and Exact Solutions for Nonlinear Reaction-Diffusion Equations Arising in Mathematical Biology," *Symmetry in Nonlinear Mathematical Physics* 1 (1997): 138–146.
[38] M. Inc, S. Hussain, A. H. Ali, et al., "Analyzing Solitary Wave Solutions of the Nonlinear Murray Equation for Blood Flow in Vessels With Non-Uniform Wall Properties," *Scientific Reports* 14, no. 1 (2024): 10588.
[39] S. Kumbinarasaiah and M. Mulimani, "A Study on the Non-Linear Murray Equation Through the Bernoulli Wavelet Approach," *International Journal of Applied and Computational Mathematics* 9, no. 3 (2023): 40.
[40] E. Hussain, A. Mutlib, Z. Li, et al., "Theoretical Examination of Solitary Waves for Sharma–Tasso–Olver Burger Equation by Stability and Sensitivity Analysis," *Zeitschrift für Angewandte Mathematik und Physik* 75, no. 3 (2024): 96.
[41] E. Hussain, Z. Li, S. A. A. Shah, E. A. Az-Zo'bi, and M. Hussien, "Dynamics Study of Stability Analysis, Sensitivity Insights and Precise Soliton Solutions of the Nonlinear (STO)-Burger Equation," *Optical and Quantum Electronics* 55, no. 14 (2023): 1274.